IEEE 2001 Ultrasonics Symposium Proceeding , pp.7-11 , paper P2B-8

APPLICATION OF MODIFIED P-MATRIX MODEL TO THE SIMULATION OF RADIO FREQUENCY LSAW FILTERS

A.N.Rusakov, V.S.Orlov, Moscow Radiocommunication Research Institute, Russia, and other.

Abstract – In designing RF filters on the basis of leaky SAW, the main challenges are decreasing insertion loss and amplitude ripples in the pass band and increasing selectivity in the stop band. Ladder resonator (LDR) filters secure the minimum insertion loss as compared with other types of RF filters. However, the amplitude ripples in the pass band are strongly dependent on losses in the resonators of LDR filters and the presence of other excited modes. The selectivity in the LDR filter stop band is determined not only by SAW resonators but also by parasitic electric elements and couplings between them both in the chip and the filter package.

In the present paper, we consider a modified P-matrix model that allows one to take comparatively simply into account resonator losses and describe LDR filters as electrical devices to make allowance for the influence of parasitic effects on their parameters. The model proposed have been used to design four RF filters for different communication systems, such as AMPS T_x 836 MHz and R_x 881 MHz; GPS R_x 1575 MHz; PCN R_x 1842 MHz.

1. INTRODUCTION

Different models describing the filter as a whole or its individual elements are used at the different stages of RF LDR filter design: electric model of the filter as a set of RLC resonators for preliminary synthesis [1]; acoustic model for the simulation of leaky SAW resonators [1]; electric macro model of the filter to take into account and compensate for parasitic elements and electromagnetic couplings in the chip and filter package at VHF [2].

The most important is the acoustic model. It connects the electrical parameters of the resonator and its layout. This model must give due consideration for various loss mechanisms in the resonators, such as propagation loss of leaky SAWs, bulk mode conversion loss at the leaky SAW reflection from electrodes etc. It is desirable that the model should take into account not only the fundamental mode but also other modes that are responsible for parasitic responses in the pass band and stop bands of the filter. At last, the model must allow the refinement of the layout of the resonators and the filter as a whole to compensate parasitic electromagnetic effects at VHF.

The classical COM or P-matrix formalisms do not take properly into account these phenomena so that various modifications of the above models have been developed [3, 4, 5, 6]. To take into consideration various loss mechanisms, we put forward a version of Morgan's P-matrix model [3].

2. MODIFIED P-MATRIX MODEL WITH LOSSES

2.1. Basic relations

The starting point of the model being described is the scattering matrix of a single electrode in the infinite periodic grating. The matrix connects radiated and incident waves (fig. 1),

$$\begin{pmatrix} b_1 \\ c_2 \end{pmatrix} = \begin{pmatrix} r & t \\ t & r \end{pmatrix} \begin{pmatrix} c_1 \\ b_2 \end{pmatrix}, \qquad (1)$$

where t and r are complex transmission and reflection coefficients, respectively.

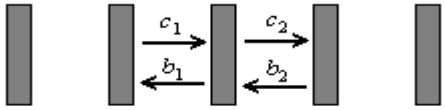

Fig.1. Wave propagation in the infinite regular grating of electrodes

If loss is not included, the law of energy conservation implies that ([1]):

$$|r|^2 + |t|^2 = 1;$$
$$t \cdot r^* + r \cdot t^* = 0 \quad \text{or} \quad |\arg r/t| = \pi/2 \qquad (2)$$

Thus, to calculate the parameters of the infinite grating one can use the absolute value $|r|$ and the effective wave velocity under grating, $V_G = (\omega \cdot p)/\arg t$, where ω is the angular frequency, p is the period of the grating. Eqs (2) are derived on the assumption that all the energy of the incident waves goes into the energy of radiated waves. With losses, this assumption becomes invalid. Losses without specification of their mechanisms can be included in Morgan's model as follows.

We consider that the power $|d_1|^2$ is scattered from the electrode at each reflection; $d_1 = \rho \cdot c_1 + \tau \cdot b_2$, where c_1 and b_2 are the amplitude of the waves incident onto the electrode. Because of symmetry, in addition to $|d_1|^2$, the power $|d_2|^2 = |\tau \cdot c_1 + \rho \cdot b_2|^2$ must also be scattered. Under such an assumption, instead of (2), we obtain the following relations

$$|r|^2 + |t|^2 + |\tau|^2 + |\rho|^2 = 1 \text{ or } |r|^2 + |t|^2 + s^2 = 1; \qquad (3)$$
$$t \cdot r^* + r \cdot t^* + \tau \cdot \rho^* + \rho \cdot \tau^* = 0 \text{ or } |\arg r/t| = (\pi/2) + A.$$

Thus, one can introduce two additional parameters to describe the characteristics of the infinite grating with due regard for losses, namely, the scattering coefficient s and the angular shift A between r and t. The A value varies within the range $|A| \le s^2/2|r|\cdot|t|$.

2.2. Effect of angular shift on the wavenumber and the reflection coefficient of the grating

According to [3,4], the dispersion equation for the wavenumber is

$$c_2 = c_1 e^{-j\gamma p};\ \ b_2 = b_1 e^{-j\gamma p},$$
$$\cos\gamma p = 1/t + t[1-(r/t)^2], \qquad (4)$$

but $r, t = f_{1,2}(|r|, V_G, s, A)$, if losses are included

Fig.2 shows dispersion dependence of $\gamma \cdot p$ calculated from (4) at different values of A. One sees that changing A decreases or increases attenuation near the reflection band of the grating and shifts the real part of the wavenumber $\mathrm{Re}\gamma$ relative to π/p. Fig. 3 shows dispersion dependence $\gamma \cdot p$ computed using FEM/BEM for 36° and 42° $LiTaO_3$ cuts (36 LT and 42 LT), where only leaky SAW propagation loss is taken into account. Comparing fig. 2 and 3 allows the suggestion that 36 LT and 42 LT mostly differ in A rather than in s.

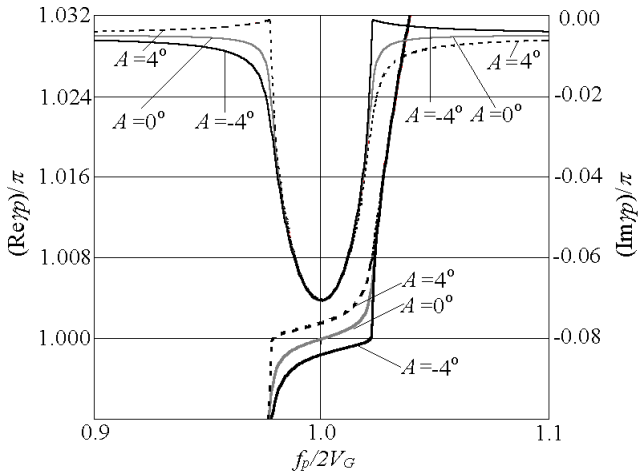

Fig.2. Frequency dependence of γp at $r = 0.07$; $s = 0.1$; $A = 0;+4°;–4°$

In our opinion, it is more convenient to analyze the frequency dependence of $\cos\gamma p$ rather than of γ. From fig. 4 one sees that $\cos\gamma p$ features the following properties. Its real part $\mathrm{Re}\cos\gamma p$ is close to a parabola, mainly dependent on $|r|$ and nearly independent of s and A. The imaginary part $\mathrm{Im}\cos\gamma p$ is practically a linear function with the slop varying as s. With no losses, $\cos\gamma p$ is real. At $A = 0$ the zero of $\mathrm{Im}\cos\gamma p$ coincides with the minimum of $\mathrm{Re}\cos\gamma p$. At $A \neq 0$ the function $\mathrm{Im}\cos\gamma p$ shifts to the right or left depending on the sign of A.

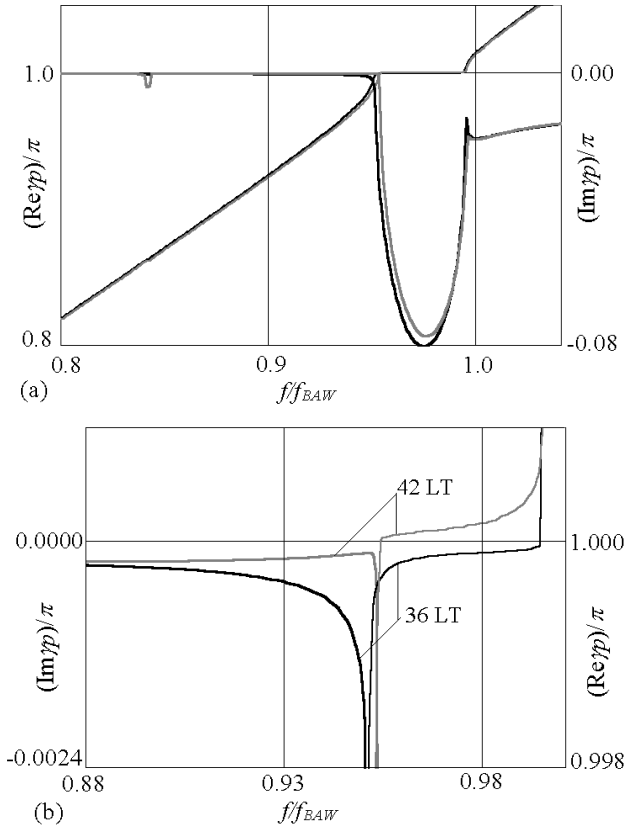

Fig.3. Frequency dependence of γp computed using FEM/BEM for 36 LT and 42 LT at Al film thickness $h/2p$ =6% and metallization ratio 0.5: (a) – wide, (b) – narrow frequency range

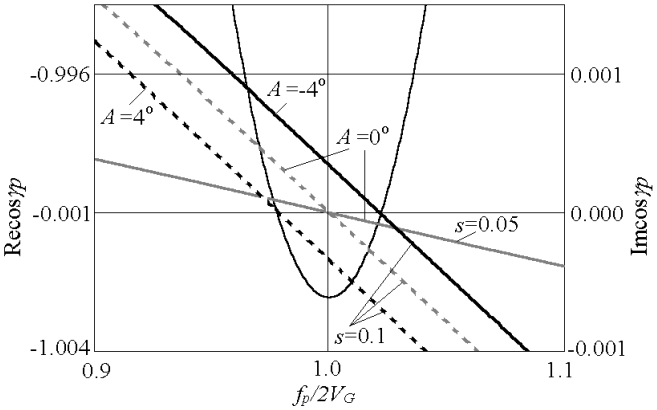

Fig.4. Frequency dependence of $\cos\gamma p$ at $r = 0.07$; $s = 0.05;\ 0.1$, $A = 0;+4°;–4°$

Fig.5 shows the frequency dependence of $\cos\gamma p$ computed using FEM/BEM for 36 LT и 42 LT; allowance is made only for propagation loss of leaky SAW. From fig. 5, the scattering coefficient s depends comparatively weakly on the thickness of Al film in the $h/2p$ range

from 2% to 6%, since the slope of $\mathrm{Im}\cos\gamma p$ is nearly alike within this range of thickness. According to our model, the main difference between 36 LT and 42 LT is in the A value, because the shift of the zero of $\mathrm{Im}\cos\gamma p$ relative to the maximum of $\mathrm{Re}\cos\gamma p$ for 36 LT and 42 LT is of different sign. It is positive for 42 LT and negative for 36 LT.

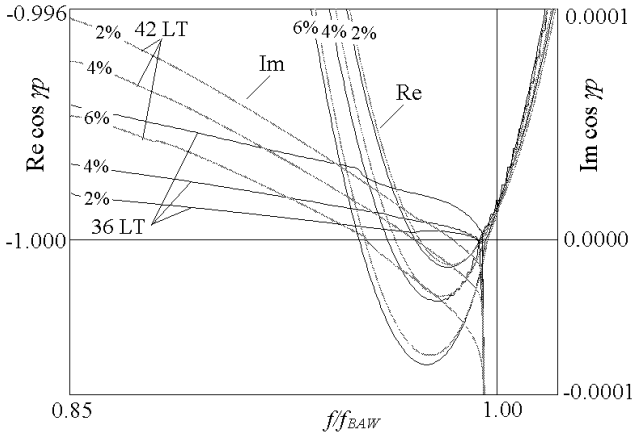

Fig.5. Frequency dependence of $\cos\gamma p$ *computed using FEM/BEM for 36 LT u 42 LT at Al film thickness* $h/2p$ *=2%, 4%, 6% and metallization ratio 0.5*

Consider the effect of the A value on the characteristics of resonators with reflective gratings of finite length. To describe resonators one uses the transfer matrix $[T_{ij}]$ or scattering matrix $[S_{ij}]$.

By analogy with [3], one obtains an analytic expression for $[T_{ij}]$ (fig. 6)

$$\begin{pmatrix} c_N \\ b_N \end{pmatrix} = \begin{pmatrix} T_{11}^N T_{12}^N \\ T_{21}^N T_{22}^N \end{pmatrix} \begin{pmatrix} c_0 \\ b_0 \end{pmatrix} \text{ or } \begin{pmatrix} b_0 \\ c_0 \end{pmatrix} = \begin{pmatrix} T_{11}^N T_{12}^N \\ T_{21}^N T_{22}^N \end{pmatrix} \begin{pmatrix} b_N \\ c_N \end{pmatrix}, \quad (5)$$

$$\|T\|^{N+1} = \|T\|^N \cdot \|T\|^1 = \|T\|^1 \cdot \|T\|^N,$$

$$\|T\|^N = \begin{pmatrix} \cos N\gamma p - S\dfrac{\sin N\gamma p}{\sin\gamma p} & R\dfrac{\sin N\gamma p}{\sin\gamma p} \\ -R\dfrac{\sin N\gamma p}{\sin\gamma p} & \cos N\gamma p + S\dfrac{\sin N\gamma p}{\sin\gamma p} \end{pmatrix},$$

where $S = 1/t - t(1-R^2)$, $R = r/t$,

$r, t = f_{1,2}(|r|, V_G, s, A)$, N is the number of electrodes.

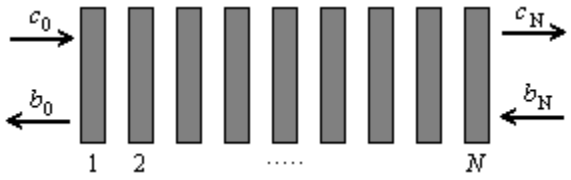

Fig.6. Wave propagation in the finite regular grating of electrodes

In fig. 7 the reflection coefficient $|S_{11}|$ calculated using (5) is given for the finite grating with N =50. The positive shift A increases $|S_{11}|$ at the left edge of the reflection band of the grating. Since the resonance frequency f_s of leaky SAW resonators for LDR filters is usually close to this edge, the Q-factor of these resonators is higher for 42 LT than for 36 LT.

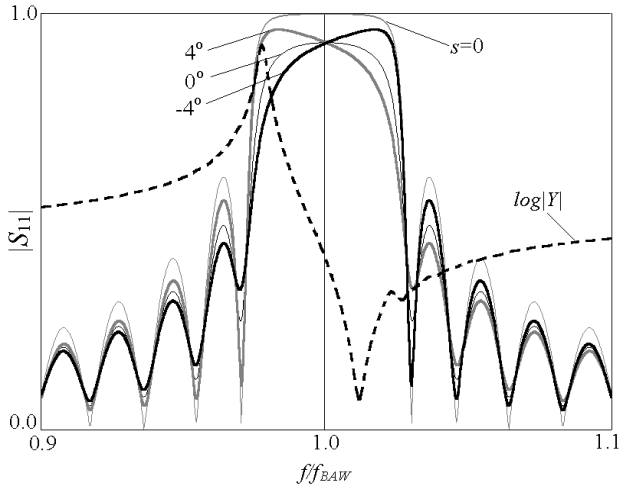

Fig.7. Reflection coefficient $|S_{11}|$ *of the grating with* N *=50 electrodes at* $r = 0.07$; $s = 0; 0.1$; $A = 0; +4°; -4°$ *and admittance* $|Y|$ *of a typical resonator.*

2.3. Estimation of electrical parameters of IDT

Now we introduce sources in the grating. Let the right-travelling a_1 and left-travelling a_2 waves are excited in the n-th gap (Fig. 8). Then

$$c_n' = c_n + a_1, \qquad b_n = b_n' + a_2. \quad (6)$$

From (5) and (6) we obtain relations for incident and radiated waves which take into account the excitation of waves in the n-th gap: if $n < m$,

$$c_m = \frac{T_{22}^{N-m}}{T_{22}^N}\left(T_{22}^n a_1 - T_{21}^n a_2\right), \; b_m = \frac{T_{12}^{N-m}}{T_{22}^N}\left(T_{22}^n a_1 - T_{21}^n a_2\right), \quad (7)$$

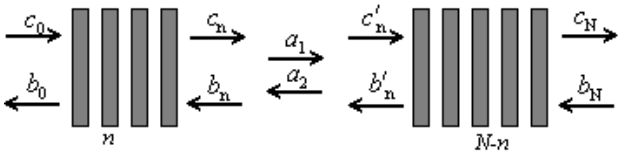

Fig.8. Wave generation in the finite grating

Eqs. (7) allow the analysis of any structure containing reflectors and sources. Analytic expressions can be derived for regular structures. For instance, the unweighted IDT with N electrodes generates the right-travelling wave

$$c_N = \frac{a_1}{T_{22}^N}\frac{\sin(N-1)\frac{Gp}{2}}{\sin\frac{Gp}{2}}\left[\cos N\frac{Gp}{2} + \frac{\sin N\frac{Gp}{2}}{\sin\gamma p}\left(S + R\frac{a_2}{a_1}\right)\right], \quad (8)$$

where $Gp = \gamma p - \pi$.

Interchanging a_1 and a_2 in (8) yields the expression for the left-emitted wave b_0 (fig. 8).

In the model [3,4], the IDT conductance $\mathrm{Re}Y_{IDT}$ is calculated using the power of the emitted waves b_0 and c_N, while the susceptance $\mathrm{Im}Y_{IDT}$ is found as the Gilbert transform of $\mathrm{Re}Y_{IDT}$. With losses, this method fails, since it does not take into account the scattering power. We propose the following method of calculating conductance.

In calculating the total impedance Y_{IDT} of IDT we use the voltage between the adjacent electrodes $U_n = V_{n+1} - V_n$ and the increment of currents $I_n = J_n - J_{n-1}$ (fig. 9). The method of estimating static capacitance is well known. Hence, we can exclude the electrostatic component from our study to consider only wave-induced currents. When the reflection coefficient $r = 0$, a good approximation for such currents is

$$J_m = DU_n e^{-jk_G p(m-n)} \quad , \; m > n \tag{9}$$

$$J_m = -D^* U_n e^{-jk_G p(n-m)} \; , \; m < n \, . \tag{10}$$

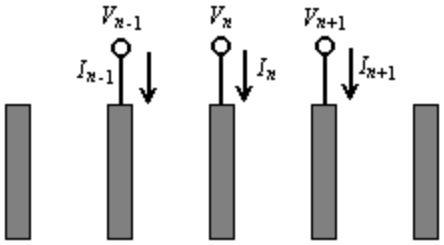

Fig.9. Generalized scheme of IDT.

Here D can be calculated using the methods of quasistatic analysis [4, 5]. This quantity becomes complex when the reflection and generation centers do not coincide. In the case of regular grating the analytic expression is known [3]. Thus, if the voltage U_n is applied to the n-th gap, there are the right-travelling wave (9) and the left-travelling wave (10). With $r \neq 0$ this waves are coupled and one can use Eqs. (1)-(8) letting

$$a_1 = DU_n \; , \; a_2 = -D^* U_n \; , \; J_m = c_m + b_m \, . \tag{11}$$

The IDT impedance can be found by summing the currents at the electrodes in the case of unit voltage applied to the IDT,

$$Y_{IDT} = \sum_{n=1}^{N} I_n V_n = -\sum_{n=1}^{N-1} J_n U_n \; ; \quad J_n = \sum_{m=1}^{N-1} (c_m + b_m) \tag{12}$$

The values of c_m and b_m are calculated from (7). Thus, double summation over electrodes is performed in (12). The simple analytic expression have been derived for the unweighted regular IDT.

Fig. 10 shows $\mathrm{Re}Y_{IDT}$ и $\mathrm{Im}Y_{IDT}$ calculated using (12) for the unweighted IDT. The conductance $\mathrm{Re}Y_p$ of the same IDT but calculated using only the power of radiated waves is also depicted. One sees that the result is substantially inaccurate if the scattered power is not taken into account.

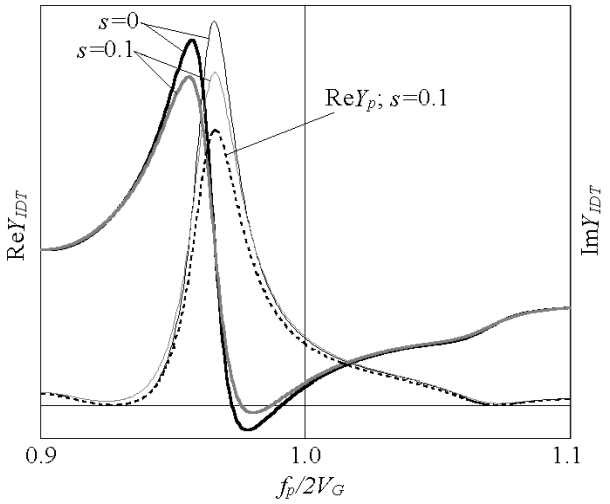

Fig.10. Impedance of unweighted regular IDT with N =30 electrodes at $r = 0.07$ and $s = 0; 0.1$

3. EXPERIMENTAL RESULTS

The above model has been applied to design a number of RF LDR filters. All the filters use yxl/42° cut $LiTaO_3$ and package SMD 3.0x3.0x1.4 mm.

Fig. 11 shows the measured response S21 of PCN R_x 1842 MHz filter. The bandwidth is BW=78.7 MHz (4.1%), insertion loss IL=1.3dB.

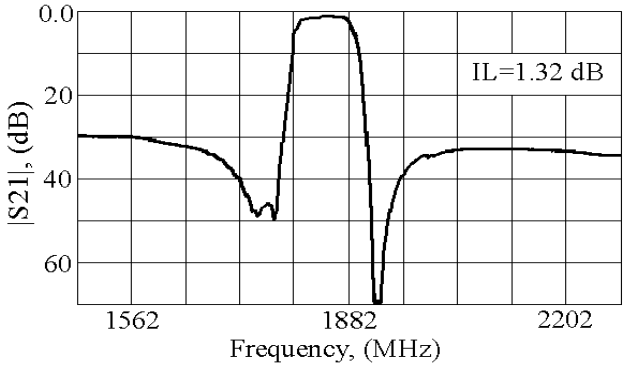

Fig.11. Measured response S21 of PCN Rx 1842.5 MHz filter

In designing RF LDR filters, the inductance of bonding wires and the capacitance of package pads must be taken into account [2]. These parasitic elements affect the filter parameters in a variety of ways. First, they change the electrical characteristics of loads at the filter input and output, i.e., to minimize losses and VSWR the filter must be designed for a track different from the 50-Ohm one. Secondly, the shunt resonators in the filter are connected with the ground bar of the package through bonding wires. The inductance of these wires changes the dynamic parameters of the resonators. Thirdly, as distinct to the filters with acoustic coupling, the input and output conductance of LDR filters can be substantially greater in the stop band and LDR filters can operate in nearly short-circuited conditions. In this case, significant currents flow

through bonding wires, increasing considerably the mutual influence of the inductance of these wires. Thus, the relative positions of bonding wires affect the frequency response of LDR filters in the stop band. To decrease electromagnetic coupling between grounded bonding wires, we have positioned these wires and grounded pads on the chip and package such that the currents in the bonding wires of the first and the second shunt resonators flowed in the opposite directions. Fig. 12 shows the responses S21 of the AMPS T_x 836 MHz filter measured and estimated without and with due regard for parasitic effects. The filter exhibits BW=35.6 MHz (4.2%) and IL=0.78 dB.

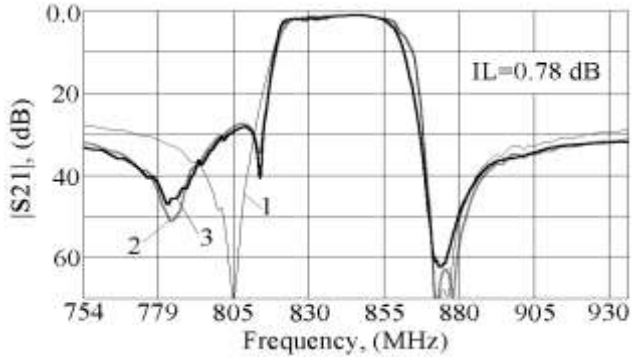

Fig.12. Simulated without parasitics (1), with parasitics (2) and measured (3) responses S21 of AMPS T_x 836 MHz filter

The influence of parasitic elements can be useful for improving the filter parameters. In this way, we achieved the selectivity greater than 50 dB in the frequency band of the transmitter T_x (from the left of the pass band) in the AMPS R_x 881 MHz filter. The parasitic inductance has been adjusted in this filter by changing the length and number of bonding wires. The responses S21 measured and estimated without and with due regard for parasitic effects are depicted in fig. 13. The filter AMPX R_x has IL=1.8 dB and BW=34.3 MHz (3.9%).

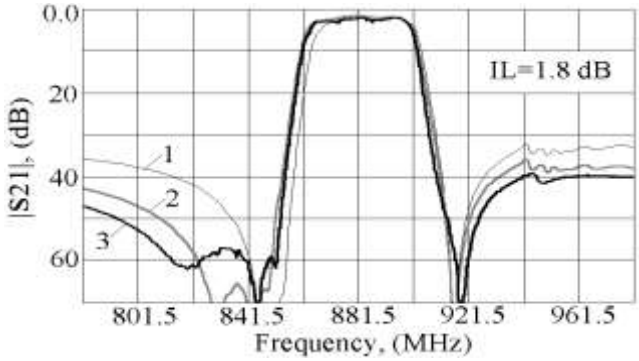

Fig.13. Simulated without parasitics (1), with parasitics (2) and measured (3) responses S21 of AMPS R_x 881 MHz filter

Extra lumped elements are required sometimes to achieve the preset parameters, e.g., to narrow the pass band and to increase selectivity. Such a necessity appeared in designing the GPS R_x 1575 MHz filter with a narrow pass band of width about BW=1% (fig.14). In the parallel arms of this filter, in addition to the resonators, extra capacitors C1 and C2 fabricated on the chip surface have been included. As a result, the filter selectivity in the stop band has increased to 45-50 dB by achieved IL=2.8 dB.

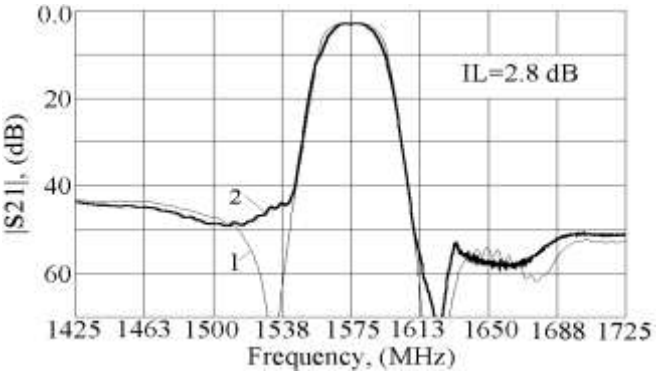

Fig.14. Simulated (1) and measured (2) responses S21 of GPS R_x 1575.42 MHz filter

4. CONCLUSION

We have considered a modified P-matrix model that accounts for loss of leaky SAW resonators in terms of the scattering coefficient s and the angular shift A between the reflection r and transmission t coefficients. On the basis of this model, simple analytic relations have been derived to estimate the characteristics of reflector and transducer gratings. This allows one to make simulation less labor consuming which is of special importance for the preliminary synthesis of LDR filters and for the subsequent analysis of the device with due regard for parasitic electromagnetic effects. The theoretical results obtained on the basis of our model are in a good agreement with the experiments for the RF LDR 836 MHz, 881 MHz, 1575 MHz, 1842 MHz filters.

REFERENCES

[1] S.Mineyoshi, O.Kawachi, M.Ueda and Y.Fujiwara, "Analysis and Optimal SAW Ladder Filter Design Including Bonding Wire and Package Impedance", IEEE 1997 Ultrason. Symp. Proc., pp. 175-178.

[2] T.Makkonen, V.P.Plessky, S.Kondratiev, and M.M.Salomaa, "Electromagnetic Modeling of Package Parasitics in SAW-Duplexer", IEEE 1996 Ultrason. Symp. Proc., pp. 29-32.

[3] D.P.Morgan, "Reflective Array Modeling for SAW Transducers", IEEE 1995 Ultrason. Symp. Proc., pp. 215-220.

[4] D.P.Morgan, "Surface-Wave Devices for Signal Processing", ELSEVIER, N-Y, 1985.

[5] P.Dufilié and P.Ventura, "Source Equalization for SPUDT Transducers", IEEE 1995 Ultrason. Symp. Proc., pp. 13-16.

[6] P.Ventura, J.M.Hodé, M.Solal, J.Desbois, J.Ribbe, "Numerical Methods for SAW Propagation Characterization", IEEE 1998 Ultrason. Symp. Proc., pp. 175-186.